Influence of ligand structure and molecular geometry on the properties of d6 polypyridinic transition metal complexes

Mauricio Arias [a], Javier Concepción [a,1], Irma Crivelli [b], Alvaro Delgadillo [a,2], Ramiro Díaz [c], Angélica Francois [c], Francisco Gajardo [a], Rosa López [a,3], Ana María Leiva [a], Bárbara Loeb [a,*]

[a] *Facultad de Química, Pontificia Universidad Católica de Chile, Casilla 306, Santiago, Chile*
[b] *Facultad de Ciencias, Universidad de Chile, Casilla 653, Santiago, Chile*
[c] *Facultad de Ciencias, Universidad Católica de Temuco, Casilla 15-D, Temuco, Chile*

Abstract

Different strategies to improve the excited state properties of polypyridinic complexes by varying ligand structure and molecular geometry are described. Bidentate and tetradentate ligands based on fragments as dipyrido[3,2-*a*:2′,3′-*c*]phenazine, dppz, and pyrazino[2,3-*f*][1,10]-phenanthroline, ppl, have been used. Quinonic residues were fused to these basic units to improve acceptor properties. Photophysical studies were performed in order to test theoretical predictions.

Keywords: dppz; ppl; Tetradentate ligand; Lifetime; Energy gap law; Quinonic fragment

1. Introduction

Transition metal complexes with polypyridines have been widely studied in the last decades mainly because of their special photophysical, photochemical and electrochemical properties. The importance of metal complexes containing polypyridine ligands, such as 1,10-phenanthroline (phen) and 2,2′-bipyridyl (bpy) in studies related to solar energy conversion, molecular electronic and light emitting devices, etc., has been well documented [1]. Although $Ru(bpy)_3^{2+}$ has concentrated much attention and undoubtedly belongs to one of the most studied compounds in chemical literature [2], research has also expanded to heteroleptic type complexes such as $[Ru(bpy)_2(N-N)]^{2+}$ (with N–N = polypyridinic ligand) and $Ru(bpy)_2X_2$ (with L = Cl−, NCS−) and also to d6 metal (e.g., Os(II) [3a] and Re(I) [3b]) polypyridinic complexes in general.

From a basic point of view, in the last years our group has been interested in understanding the processes that occur after light excitation of these type of complexes, and therefore those that govern excited state behaviour and decay. One of the main goals has been to analyze the factors that enhance excited state lifetime. Two main aspects were considered: the nature of the *acceptor ligand* and the *geometry of the complex*. In this article, part of this work is reported.

2. Acceptor ligand

There is abundant literature on metal to ligand charge transfer (MLCT) excited states in d6 polypyridinic complexes, and much progress has been achieved in the understanding of variables such as electronic structure and medium effects [4]. An important molecular feature

in these excited states is the acceptor ligand, the ultimate ligand of residence for the excited electron. In heteroleptic chelates, this is the ligand having the lowest π^* acceptor level [5]. Manipulation of the acceptor ligand can be used to control excited state lifetime.

2.1. Influence of the acceptor ligand properties on the lifetime: energy gap law

Most polypyridyl complexes of Ru(II), Os(II), and Re(I) are sufficiently weak emitters that lifetimes are dominated by nonradiative decay, i.e., the lifetime (τ) value is mainly governed by the non-radiative rate constant, k_{nr}:

$$\tau^{-1} \sim k_{nr}. \tag{1}$$

Nonradiative decay from MLCT states to the ground state is typically dominated by energy loss into a series of medium-frequency ring stretching vibrations with energy spacing between 1000 and $1600 \, cm^{-1}$ [5,6]. It is usually considered that these vibrations can be approximated as a single averaged mode of quantum spacing $\hbar\omega_M$ and electron-vibrational coupling constant S_M. This latter term is related to the change in equilibrium displacement between ground and excited state, ΔQ_e, and the reduced mass M by

$$S_M = \frac{1}{2} \frac{M\omega}{\hbar} (\Delta Q_e)^2. \tag{2}$$

In the limit where E_0, the energy gap, is $E_0 \gg S_M\hbar\omega_M$, and $\hbar\omega_M \gg k_BT$, k_{nr} varies with E_0 according to the energy gap law, Eq. (3). The complete development of the energy gap law is reported elsewhere [5,6]. For practical reasons, it can be shown that the main contribution to k_{nr} arises from a linear term, the energy gap term, and therefore the energy gap law can be approximated to:

$$\ln \tau^{-1} \sim \ln k_{nr} \propto -\frac{\gamma E_0}{\hbar\omega_M}. \tag{3}$$

Analysis of lifetimes based on the energy gap law is valid only for nonradiative decay from the lowest MLCT state or states. The relationship between k_{nr} and the energy gap E_0 given in Eq. (3), has been shown to be valid for MLCT decay in many cases, not only for Ru(II) polypyridine compounds, but also for Os(II) and Re(I) [7]. For the latter metal ion, tricarbonyl polypiridinic complexes have been mostly studied [7b]. Nevertheless, the acceptor ligand appears in two different ways in Eq. (3). One is the energy gap E_0 mentioned above. The other is the extent of excited state distortion, as measured by ΔQ_e, Fig. 1a [7g]. According to Eq. (2), ΔQ_e relates to S_M, which in turn relates to the γ parameter in Eq. (3) through:

$$\gamma = \ln \left(\frac{E_0}{S_M\hbar\omega_M} \right) - 1. \tag{4}$$

These parameters dictate the magnitude of vibrational wave function overlap between $v'_M = 0$ levels in the excited state and $v_M = 0, 1, 2, \ldots$ levels in the ground state, Fig. 1b. A small overlap will contribute to diminish k_{nr} and there-

fore increase τ. In the limit where the energy gap law is valid, overlap diminishes as E_0 increases. Nevertheless, overlap also diminishes as S_M decreases. Therefore, a combination of rigidity and delocalization may help to obtain enhanced lifetimes. The larger the molecular framework where the electron can delocalize in the excited state, the less displacement changes in local C–C and C–N bonds will be observed. Consequently, ΔQ_e will be smaller, as well as k_{nr}. Rigidity also diminishes ΔQ_e with the same effect.

A role for ligand rigidity and S_M has been found in comparing osmium complexes with bpy and phen as acceptor ligands. $[Os(bpy)_3]^{2+*}$ and $[Os(phen)_3]^{2+*}$ have comparable energy gaps ($E_0 \sim 13{,}400 \, cm^{-1}$), but k_{nr} for the bipyridine complex is approximately four times that of the phenanthroline complex in acetonitrile at 298 K [5,11]. Franck–Condon analysis of emission spectra demonstrated that $S_{phen} < S_{bpy}$, i.e., $\Delta Q_{e\,phen} < \Delta Q_{e\,bpy}$, reflecting the enhanced rigidity in phenanthroline as the acceptor, arising from the chemical link between the pyridyl ligands [5].

In this line of thought, ligands (N–N) = dpp′, ppl, dpq′ and dppz, Fig. 2a, where chosen as acceptor ligands.[4] They were used in complexes of type $[Ru(N-N)_3]^{2+}$, $[Ru(bpy)_2 (N-N)]^{2+}$ and $[Re(N-N)(CO)_3L]^{+/0}$, with L = Cl⁻, OTf⁻ or substituted pyridines. Table 1 summarizes some spectroscopic results.

From Table 1, it can be observed that as the number of rings in the acceptor ligands is increased, the energy gap (considering $E_0 \sim E_{em}$) decreases. For example, for the $[Ru(bpy)_2(dpp)](PF_6)_2$ and $[Ru(bpy)_2(dpq)](PF_6)_2$ complexes, where dpp and dpq are the corresponding acceptor ligands, E_{em} varies from 15,152 to $13{,}055 \, cm^{-1}$. The decrease in the energy gap occurs because of stabilization of the lowest π^* acceptor level, as shown by electrochemical measurements: -0.96 V for the dpp complex and -0.75 V for the dpq complex (vs. SCE in acetonitrile) [7i–k]. The $Ru^{3+/2+}$ process remains nearly constant for both complexes [5]. A similar tendency can be observed when comparing $[Ru(bpy)_2(dpp')](PF_6)_2$ and $[Ru(bpy)_2(dpq')]$ $(PF_6)_2$. More dramatic effects emerge when $[Ru(bpy)_2 (dpp)](PF_6)_2$ and $[Ru(bpy)_2(dpp')](PF_6)_2$ are compared. Although the energy gap (reflected in E_{em}) diminishes from the complex with dpp to the complex with dpp′, the lifetime is strongly enhanced, from 216 to 1214 ns, due to the enhanced delocalization possibilities in the latter. The same tendency, although less dramatic, is observed when comparing $[Ru(bpy)_2(dpq)](PF_6)_2$ and $[Ru(bpy)_2(dpq')](PF_6)_2$. A combination of rigidity *and* delocalization may account for the enhanced lifetimes. Delocalization plays a role, as evidenced by the decrease in emission energies. Nevertheless, the bipyridine versus phenanthroline comparison

---

[4] There is some confusion in regard to the abbreviation of nomenclature for some of these ligands. dpq′ has also been denominated ppb (Ref. [8]) while ppl has been called DPQ (Ref. [9]) and dpp′ was formerly named ppz (Ref. [10]).
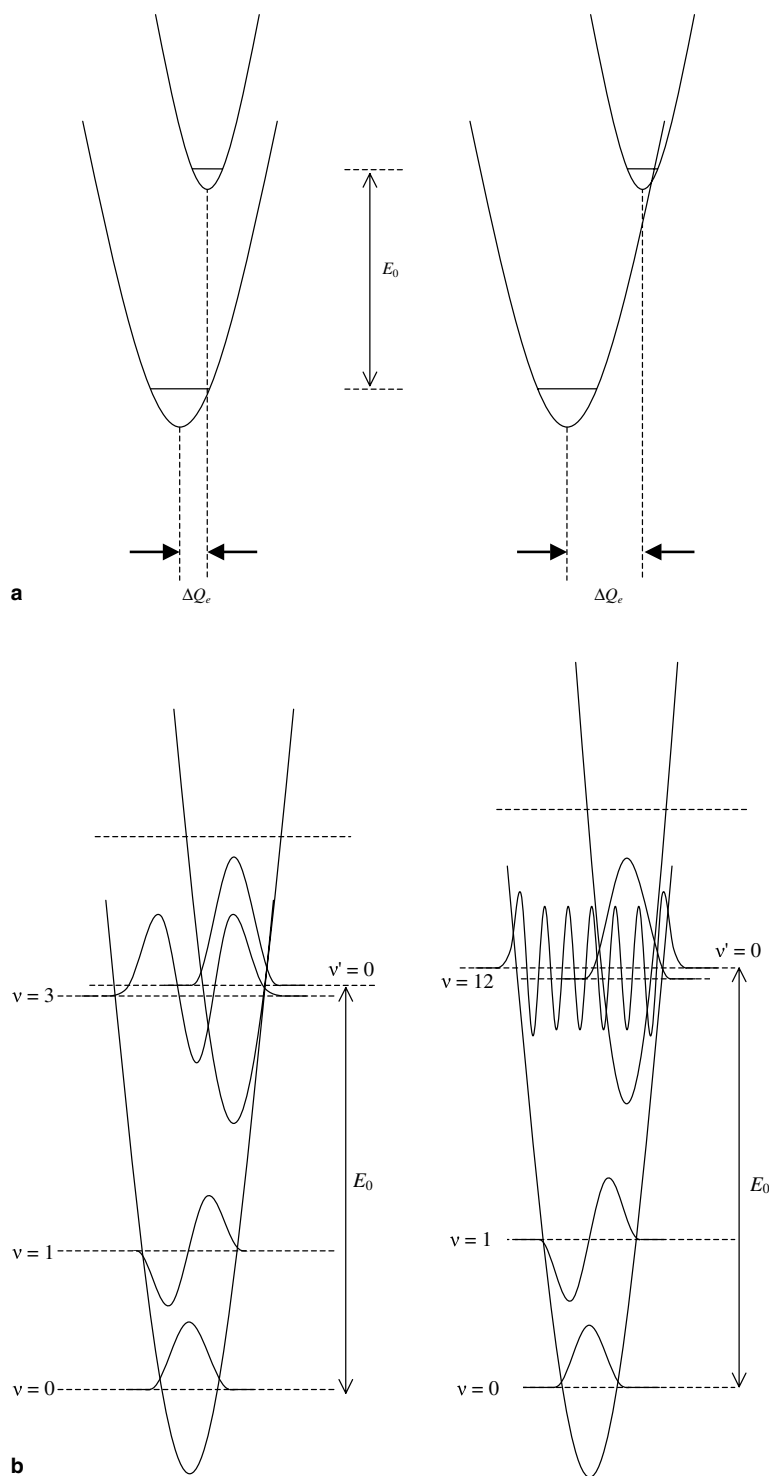
Fig. 1. (a) E_0 and ΔQ_e energy gap law parameters, (b) vibrational wave function overlap.

mentioned above for Os^{2+} complexes, suggests that the additional bond linking the ring systems in dpp′ and dpq′ may play a role as well, diminishing ΔQ_e, and consequently S_M and k_{nr}.

For the $Re(N–N)(CO)_3Cl$ series of complexes reported in Table 1, the decay is governed by the E_0 parameter. The additional ring in dppz in regard to ppl stabilizes the

π^* level: the energy gap and consequently the lifetime diminishes, following the energy gap law. Nevertheless, when N–N = Me₂dppz, the lifetime is notably enhanced compared to that of N–N = dppz. Variables different to the energy gap law could be responsible of the mentioned behaviour. Specifically, it has long been discussed that in Re(I) polypyridyl complexes there is an interplay between

(a)

bpy   phen   dpp   dpp'   Rppl R = H, CH$_3$ (Me), COOCH$_2$CH$_3$ (e)

dpq   dpq'   Rdppz R = H (dppz), Me (Me$_2$dppz)
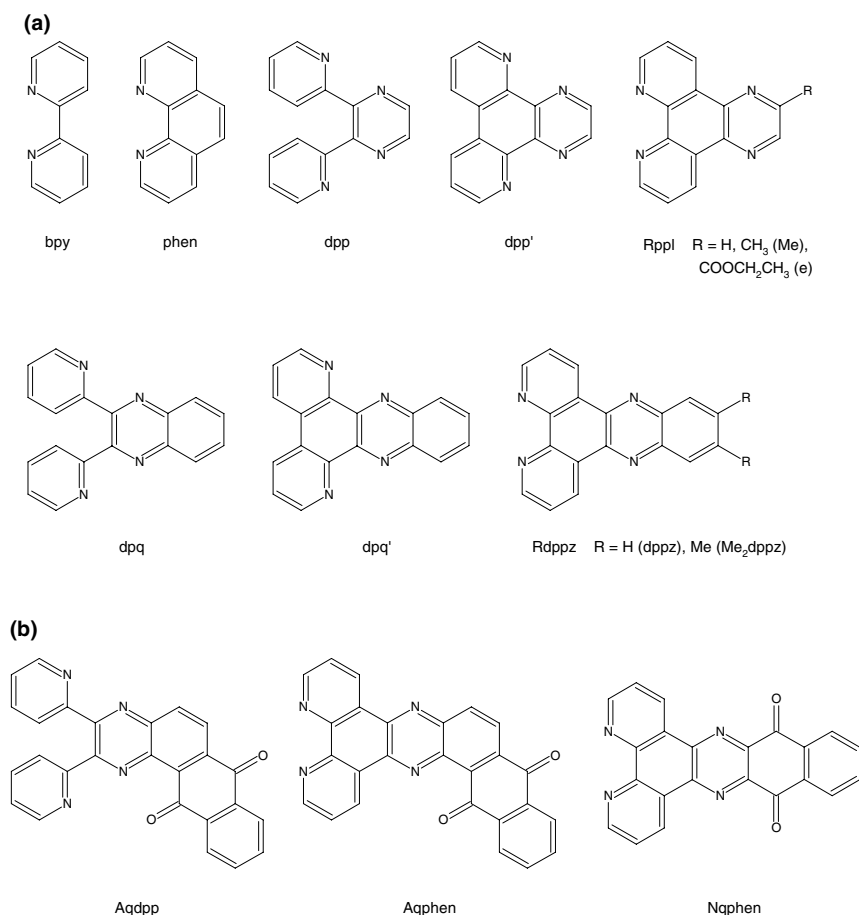
(b)

Aqdpp   Aqphen   Nqphen

Fig. 2. (a) Ligand structures and (b) molecular skeleton for the quinonic acceptor ligands Aqdpp, Aqphen and Nqphen.

Table 1
Ground and excited state parameters for Ru^{2+} and Re^{+} polypyridyl complexes at 298 K

Complex	λ_{abs} (nm)	λ_{em} (nm)	τ (ns)	ϕ_{em}	E_{em} (cm^{-1})	Reference
[Ru(bpy)$_3$](PF$_6$)$_2$	452	620	910	0.062	16,129	[1a,1c]
[Ru(dppz)$_3$](PF$_6$)$_2$	442	618	770	–	16,181	[8l]
[Ru(ppl)$_3$](PF$_6$)$_2$	455	606	519	0.039	16,502	[7h]
[Ru(Meppl)$_3$](PF$_6$)$_2$	453	602	584	0.033	16,584	[7h]
[Ru(eppl)$_3$](PF$_6$)$_2$	455	603	517	0.037	16,584	[7h]
[Ru(bpy)$_2$(dpp)](PF$_6$)$_2$	464	660	226	0.049	15,152	[7j,7k]
[Ru(bpy)$_2$(dpp′)](PF$_6$)$_2$	466	678	1214	–	14,749	[10a]
[Ru(bpy)$_2$(dpq)](PF$_6$)$_2$	516	766	71	–	13,055	[7j,7k]
[Ru(bpy)$_2$(dpq′)](PF$_6$)$_2$	536	828	327	–	12,077	[10a]
[Ru(bpy)$_2$(ppl)](PF$_6$)$_2$	454	630	955	0.022	15,873	[7h]
[Ru(bpy)$_2$Meppl](PF$_6$)$_2$	455	630	995	0.062	15,873	[7h]
[Ru(bpy)$_2$(eppl)](PF$_6$)$_2$	460	647	930	0.068	15,456	[7h]
Re(bpy)(CO)$_3$Cl	370	633	50	0.0035	15,798	[7b,7i]
Re(ppl)(CO)$_3$Cl	380	628	83	–	15,924	[13f]
Re(dppz)(CO)$_3$Cl	378	649	38	0.001	15,408	[7i]
Re(Me$_2$dppz)(CO)$_3$Cl	387	640	913	0.0086	15,625	[7i]
Re(dpp)(CO)$_3$Cl	406	700	<20	0.00014	14,286	[7b]

lowest lying MLCT and ligand localized $^3\pi$–π^* excited states [8b,8c]. In the case of Re(X$_2$-dppz)(CO)$_3$Cl (X = H, CH$_3$, Cl), it was demonstrated that $^3\pi$–π^* lie lowest, but low energy MLCT states can be populated at room temperature and dominate emission and excited state decay [8d,8e]. Lifetime is deeply enhanced when $^3\pi$–π^* transitions are involved, and this may be the case in Re(Me$_2$dppz) (CO)$_3$Cl. It must be commented at this point that Blackman and co-workers [8h] report an extremely long lived excited state (2 µs) for [Cu(11-Br-dppz)(PPh$_3$)$_2$](BF$_4$). The emission spectra suggest a MLCT origin for it, as they are completely quenched in methanol.

Summing up, delocalization and rigidity permit to enhance excited state lifetime, even at the cost of a smaller energy gap. The subsequent work mainly concentrated on two of these ligands, dppz and ppl. Taking into account that these type of ligands are additionally interesting from the perspective of their electronic structure [8h,8g], a deeper study of this aspect was considered.

2.2. Electronic structure in the dppz and ppl ligands

The ligand dppz, is widely discussed in the literature [8] while references for ppl are rather scarce [9]. These ligands are easily obtained through a condensation reaction of the type shown in Scheme 1 [9a,12].

The ligand dppz can be considered to be constituted by two fragments, 2,2′-bipyridine and phenazine, Scheme 2. In the same way, ppl can be considered as based on the 2,2′-bipyridine and quinoxaline fragments.

Bringing the fragments together results in an electronic rearrangement in the ground state that is reflected in the ^{1}H NMR resonances. All the protons of the bipyridine fragment shift low field. The effect is mostly evident for the *ortho* and *para* protons. Specifically, for both ligands the *ortho* proton is shifted low field in 0.74 ppm in regard to free bpy. In the case of the *para* proton, the displacement is 1.85 ppm for ppl and 1.89 ppm for dppz. The enhanced effect is due to the proximity of the pyrazine nitrogen, wich of its anisotropy generates a favorable magnetic field for the resonance of the mentioned protons. The greater effect observed for the second is attributed to an electronic rearrangement produced by the presence of an additional ring. This electronic reorganization is also observed in phenazine

and quinoxaline fragments: on going from the free fragment to the full ligand, a displacement from 8.85 to 9.0 ppm is observed for ppl, and from 8.25 to 8.36 ppm and 7.83–7.93 ppm for dppz. To analyze the effect of a substituent in the pyrazine (dppz) and quinoxaline (ppl) fragments, a study was carried out with substituents of donor or acceptor capacity [9a,17b].

The presence of a substituent on the * marked position on dppz, Scheme 2, causes a loss in symmetry as compared to unsubstituted dppz [17a]. The magnetic inequivalence thus introduced affects the phenazine fragment protons and the bpy protons, although to a different extent. The phenazine protons close to the substituent are more affected, as expected. As the donating properties of the substituent increase a high field displacement is observed, following the trend:

$$NO_2 < COOH < H < CH_3 < NH_2.$$

For the protons at both sides of the substituent position, a very good correlation was observed between the protons chemical shift and the calculated total charge on the carbon atoms bound to the protons. The variation of the chemical shifts of these protons by varying R was interpreted as an electronic effect, induced by the electron withdrawing or electron donating capacity of the substituent. No such correlation was observed for the *meta* proton, pointing out that its behaviour must arise from different effects than merely electronic. An effect due to the anisotropy of the neighboring phenazine ring heteroatomic N atom was invoked. A similar trend was observed for R–ppl ligands, with R representing the substituent on the * position (Scheme 2) of the ligand [9a]. As expected, the signal corre-
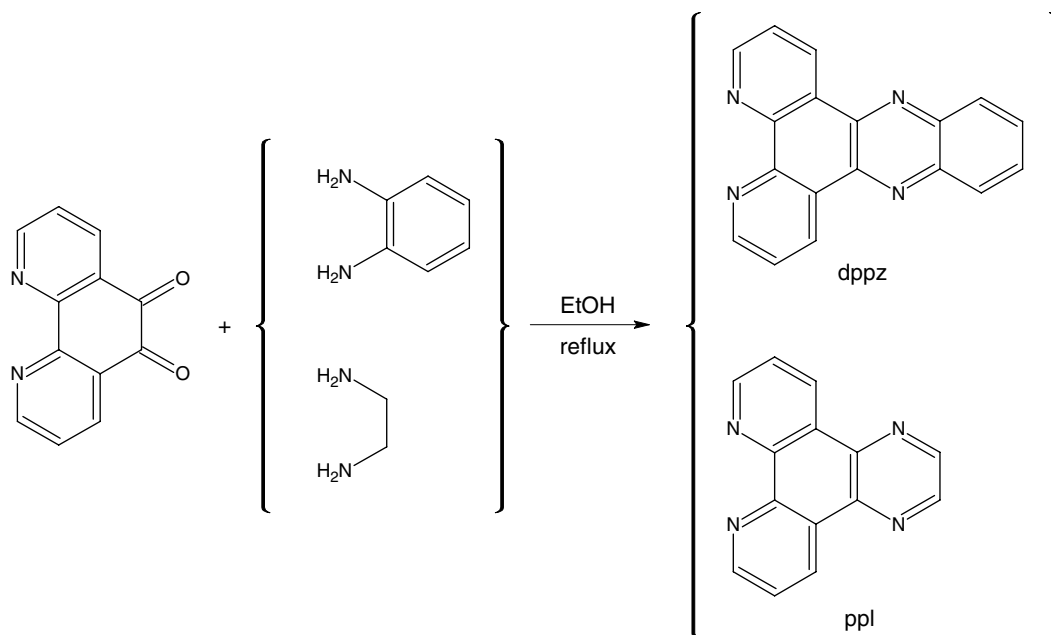
Scheme 1.
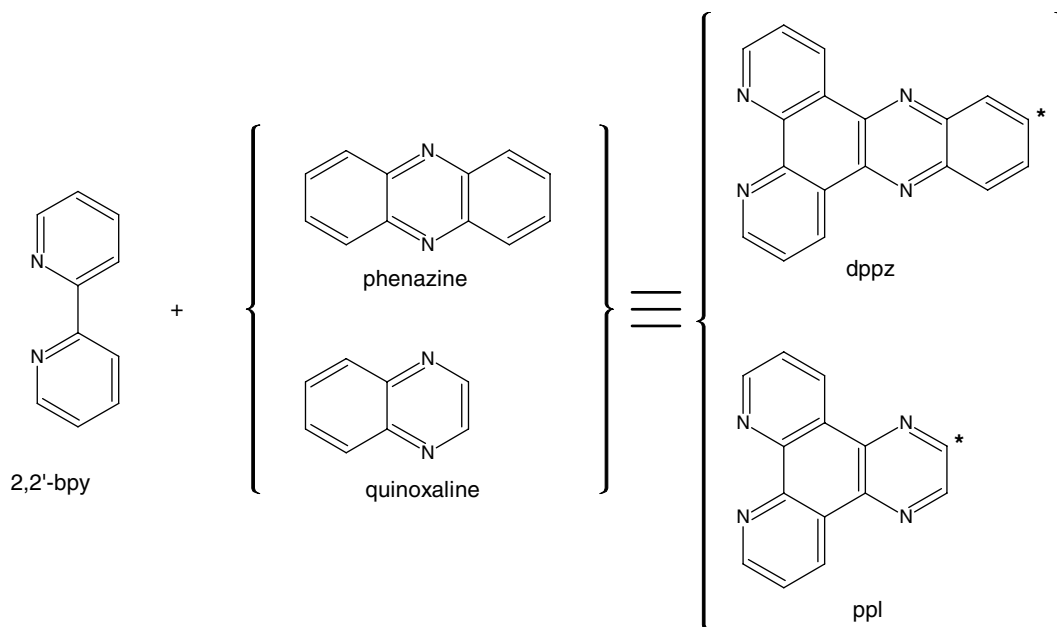
Scheme 2.

sponding to the quinoxaline proton is strongly affected by the nature of the substituent. If R = Me, its shielding is enhanced (0.2 ppm) compared to ppl, whereas if R = COOMe, this proton is manifestly unshielded (0.8 ppm) due to the electron-acceptor properties of the ester group.

The properties of the dppz ligand suggest that on reduction it tends to form a radical anion with the charge located on the phenazine portion of the ligand, as pointed out by Kaim and co-workers [8k,8l], Gordon and co-workers [8h], and others. EPR studies on this ligand corroborate this hypothesis [13c]. The excited state of dppz complexes also shows interesting effects, as described in Section 2.1 for the rhenium complexes of substituted dppz. Complexes with ligands such as dppz and ppl show other attractive properties, e.g., light switch effects [8f], applicability in organic light emitting devices (OLEDs) [8j], or DNA intercalation [8i]. The light switch effect, i.e., luminescence in aprotic solvents or when bound to DNA, and non-emission in water, was observed for [Ru(bpy)$_2$dppz]$^{2+}$, and its behaviour reinterpreted by Meyer and Papanikolas. Their study supports also the view of bpy and phenazine differentiated states associated with the dppz ligand. The bpy fragment is associated with a ''bright'' state similar in properties than the MLCT state in Ru(bpy)$_3^{2+}$. The ''dark'' state would be mainly located on the phenazine portion. The light switch effect, formerly thought to be driven by

a state reversal of two MLCT states on the ligand, was interpreted as being due to the dark level being always lowest. The light switch effect would be a result of a competition between energetic factors that favor the dark state and entropic factors that favor the bright state. Very recently, a theoretical study for the same complex was reported [17c]. It was found that the solvent effects are critical in understanding the nature of the excitations. A state reversal between a dark $^3\pi$–π^* level and ^{3}MLCT between Ru and dppz was again invoked.

Considering their special properties and potentiality, dppz and ppl were taken as basic structures to build more sophisticated ligands, as described in the following paragraphs.

2.3. Enhanced acceptor properties in dppz and ppl type ligands

One additional step to achieve long-lived excited states was to obtain bidentate chelating ligands with substituents that posses strong acceptor capacity. Therefore, the synthesis of ligands that incorporate quinonic groups in non-coordinating positions was carried out. The idea is that the presence of the acceptor groups should help to separate the positive and negative centers, and therefore, difficult back charge recombination after MLCT excitation, Scheme 3.
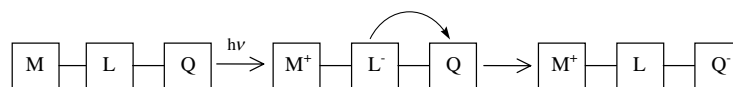
Scheme 3.

There are examples in the literature of bpy type ligands substituted with deactivating quinonic groups [14]. When these ligands are coordinated to Ru(II) or Re(I), an excited state quenching process is observed with little, if any, emission. The formation of a charge separated excited state explains this behaviour. The ligands cited, all show a *pendant* quinonic group, joined to the bpy framework through a single bond. In order to add delocalization and rigidity, the ligands designed in our group used dppz or ppl as base, with the quinonic fragment *fused* to the molecule. The ligands synthesized were 2,3-di(2-pyridyl)naphtho[2,3-*f*]quinoxaline-7,12-quinone, Aqdpp [13a], 12,17-dihydro-naphtho [2,3-h]dipyrido[3,2-a;2′,3′-*c*]phenazine-12,17-dione, Aqphen [13b,13c], and dipyrido[3,2-a;2′,3′-*c*]-benzo[3,4]-phenazine-11,16-quinone, Nqphen [13d], Fig. 2b.

The ligands can be visualized as a polypyridinic fragment (dpp, dppz and ppl, respectively) "fused" with a quinonic tail. Aqphen is therefore more rigid than Aqdpp, in the same way as discussed for dpp and dppz above. Nqphen has the property of being more linear than the other two.

The general synthetic method to obtain Aqdpp, Aqphen and Nqphen is based on a similar condensation reaction as that described in Scheme 1 for dppz and ppl. The condensation was verified in all cases by the disappearance of the carbonyl tension bands of the corresponding dione (at ∼1700 cm^{-1}), and the NH tensions of the condensing diamino compound (∼3500 cm^{-1}). NMR characterization and elemental analysis permitted to verify the nature of the ligands. In the case of Aqphen, the insolubility of the ligand generated a badly resolved ^{1}H NMR spectrum. The neutral (Aqphen)Re(CO)$_3$Cl compound permitted a better resolution. In the spectrum for Aqdpp the pyridyl ligand signals superimpose with the quinone ring protons. Nevertheless, the structural differ-

ence between the more rigid and delocalized Aqphen and the more flexible Aqdpp can be clearly observed on the quinoxaline fragment. Both, Aqdpp and Aqphen, show the same effect observed than the one described for dppz. For Aqdpp and Aqphen, the UV–Vis absorption spectrum is dominated by the characteristic anthraquinone absorption bands [13e] between 380 and 400 nm. In Nqphen the corresponding bands are displaced to higher energies. The molecular structure of Aqdpp was determined by X-ray diffraction [13a]. The anthraquinone–diazine entity is quite planar with a maximum deviation of 0.138(4) Å from the best mean plane. The pyridine groups, are oriented out of plane with dihedral angles of 57.0(2)° between each other and angles of 132.8(1)° and 144.4(2)° with respect to the pyrazine ring. Theoretical structural and electron density calculations where also performed. Semiempirical methods at PM3 level permitted to obtain the molecular structure in the gas phase. Close similarity to the crystal structure was observed, except that the anthraquinonic part in the calculated structure (gas phase) is considerably more bent at the central ring than in the crystal, with a distortion angle of 35.8°. Nevertheless, both structures show that the –C=O groups of the quinonic region are out of plane. Regarding the electronic distribution in the molecular frontier orbitals, the HOMO shows high electronic density on the pyrazine fragment of the ligand, while in the LUMO the electronic density lies mainly on the quinonic region of the anthracene fragment. Only one pyridyl ligand has some contribution to the HOMO, Fig. 3. As can be seen also in Fig. 3, the HOMO and LUMO of Aqphen have a similar pattern, although in the latter case a strong contribution to the HOMO from the phenanthroline part of the ligand is observed. In the case of Nqphen a similar pattern is exhibited, although in this
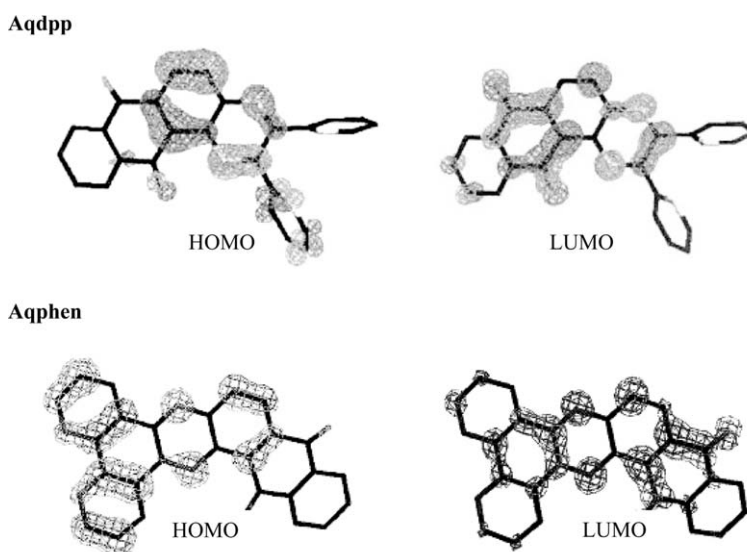

Fig. 3. Electronic distributions for the HOMO and LUMO for Aqdpp and Aqphen.

case an enhanced contribution of the pyrazine region to the LUMO is observed.

The acceptor properties of the ligands are evidenced by cyclic voltammetry, where reduction processes at a less negative potential than that normally observed for bpy or phen type ligands, occur. Two distinct reductions were observed in this region for Aqdpp and Aqphen. The first (–0.64 V for Aqdpp and −0.5 V for Aqphen) is reversible, and was attributed to the formation of the semiquinone, while the second (−0.86 V for Aqdpp and −0.8 V for Aqphen) is irreversible and probably related to the formation of the dianion. In Nqphen it is difficult to separate both processes, and a broad reduction signal at −0.708 V was detected. These assignments are supported by EPR measurements. The Aqphen ligand was chemically reduced with potassium *t*-butoxide in DMSO [13c]. The splitting observed in the EPR spectrum corresponds to a quinone-based reduction with the unpaired electron interacting with one hydrogen of the pyrazine region of the molecule, H8, and a pair of equivalent hydrogens of the benzene ring close to the quinonic region (H9 and H12), Fig. 4a. The simulated spectrum is shown in the inset. This simulation gave $a_H = 0.51$ mT, $a_{2H} = 0.15$ mT and $a_{2H} = 0.21$ mT. The EPR spectrum shown for Aqphen is notably different than that for dppz [13c]. The ligand dppz can be visualized as the polypyridinic fragment of Aqphen, without the qui-

nonic portion. For the reduced dppz, the interaction between the added electron and two equivalent nitrogen atoms on the phenazine portion of the ligand was detected, with a coupling constant of 0.56 mT. The EPR for reduced Nqphen, Fig. 4b [13f], shows very little resolution and broad bands. Based on the mentioned electrochemical results, where a single broad signal was observed for the reduction to semiquinone and subsequently to the dianion, indicating the proximity of the potential of both reduction processes, the low defined pattern observed was attributed to the presence of an equilibrium between the paramagnetic semiquinone and the diamagnetic dianion. The simultaneous presence of a paramagnetic and a diamagnetic species would be responsible for the broadening and lack of resolution observed. The model fragment for Nqphen is ppl. The EPR of ppl·⁻ shows a characteristic pattern for a system with a high degree of delocalization, with the added electron interacting with all the nuclei of the ligand. Nevertheless, the coupling constants indicate that the pyrazinic region, especially the pyrazine nitrogens, concentrate a higher electronic density than the rest of the molecule [13f]. The results are in agreement with the HOMO orbital description given above.

Rhenium complexes of the type *fac*-[(AL)Re(CO)$_3$L]$^{+/0}$, with AL = Aqphen or Nqphen, and L = Cl$^-$, OTf$^-$, or a substituted pyridine, were obtained and characterized [13b–d]. A full identification of a charge separate state was achieved for *fac*-[(Aqphen)Re(CO)$_3$py-PTZ]$^+$ [13c], with py-PTZ = 10-(4-picolyl)phenothiazine, a known donor molecule [15]. The complex *fac*-[(Aqphen)Re(CO)$_3$py-PTZ]$^+$ shows no emission. It must be mentioned that, with the sole exception of *fac*-[(Aqphen)Re(CO)$_3$(OTf)], which displays a very weak emission at 525 nm in 1,2-dichloroethane at 298 K with $\tau < 20$ ns, all the compounds of the type *fac*-[(Aqphen)Re(CO)$_3$L]$^{+/0}$, with L = Cl$^-$, 4-ethylpyridine, etc., show no emission. Considering that the corresponding model complexes *fac*-[(dppz)Re(CO)$_3$L]$^{+/0}$ emit [16], this behaviour can be interpreted as a preliminary evidence of the quenching acceptor properties of Aqphen. The transient absorbance difference (TA) spectrum of *fac*-[(Aqphen)Re(CO)$_3$py-PTZ]$^+$ is shown in Fig. 5.

At 20 ns, three new features are evident, with a decay of $\tau = 300$ ns ($k = 3.33 \times 10^{-6}$ s^{-1}), independent of the monitoring wavelength. First, a signal at 560 nm can be observed. This feature is also present in the TA spectra of the corresponding complexes with L = OTf$^-$ and 4-Et-py. It was assigned to a $\pi \rightarrow \pi^*$ transition localized on the reduced Aqphen [13c], since an absorption band at this same wavelength appears in the spectrum of electrochemically generated Aqphen·⁻ [13b]. Characteristic bands for PTZ·⁺ were also detected in the TA spectrum of *fac*-[(Aqphen)Re(CO)$_3$py-PTZ]$^+$ at 475 and 510 nm. With the TA analysis, the electronic movement on the ligands in the excited state(s) is therefore evidenced. Complementarily, ground state and time-resolved infrared (TRIR) absorption difference spectra for *fac*-[(Aqphen)Re
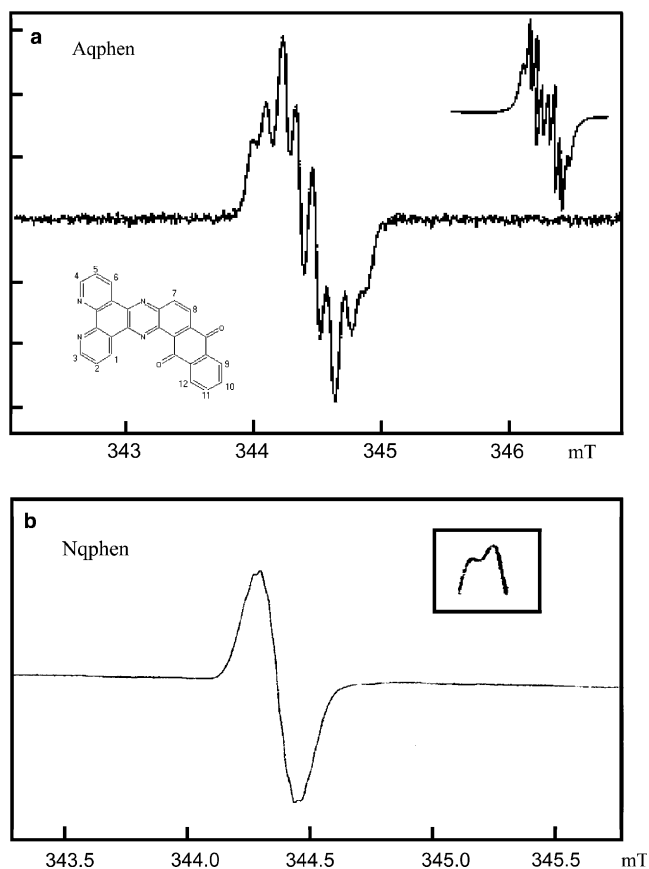

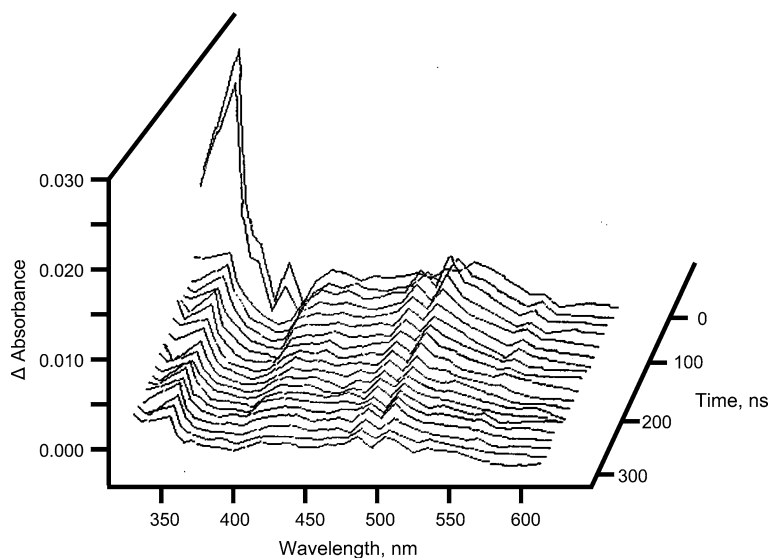Fig. 4. EPR spectra for (a) Aqphen·⁻ and (b) Nqphen·⁻, in DMSO.

Fig. 5. Transient absorption difference (TA) spectra for *fac*-[(Aqphen)Re(CO)₃py-PTZ]⁺ in 1,2-DCE from 0 to 300 ns at 20 ns intervals [13c].

(CO)₃py-PTZ]⁺ shed light on electronic aspects related to the rhenium metal center. In the ground state spectrum, ν(CO) bands appear at 2040, 1938 and 1932 cm⁻¹, assigned to A′(1), A′(2) and A″ in pseudo-C_{3v} symmetry. A quinone band appears at 1678 cm⁻¹. In the TRIR difference spectrum, the ν(CO) bands are shifted to 2034, 1935 and 1917 cm⁻¹, and the quinone band to 1560 cm⁻¹. The slight shift of the ν(CO) is much smaller and in opposite direction than the one observed for MLCT bands. The small shifts in the photochemical transient show that the electron density at the metal is relatively unperturbed compared to the ground state [20]. In this way, the presence of a charge separate state in the excited state was fully proved. The PTZ fragment introduces a new step to the mechanism proposed in Scheme 3. Specifically, the presence of a donor produces an excited state with the charges separated at a longer distance. Therefore, longer lived excited states are expected. This strategy is shown in Scheme 4.

One important point is that for the series of complexes *fac*-[(L-L)Re(CO)₃py-PTZ]⁺, with (L–L) = bpy, dppz and Aqphen, the recombination constant is 4.0×10^7 s⁻¹, 9.1×10^6 s⁻¹ [21], and 3.3×10^6 s⁻¹, respectively. The effect of delocalization and rigidity on going from bpy to dppz, and the additional *fused* quinonic moiety in Aqphen

prove therefore their role in enhancing the excited state lifetime.

3. Geometry of the complex

3.1. cis vs. trans geometry in $[Ru(N\text{–}N)_2L_1L_2]^{0,n+}$ type complexes

As mentioned in the former paragraphs, ruthenium polypyridyl complexes of the type $[Ru(N\text{–}N)_2L_1L_2]^{n+}$ (N–N) = 2,2′-bipyridine, 1,10-phenanthroline, or similar, $L_1 = L_2$, or $L_1 \neq L_2$, have been widely studied. Most of the work reported until now is related to $[Ru(N\text{–}N)_2L_1L_2]^{0,n+}$ complexes having *cis* geometry, reflecting a definite preference of *cis* over *trans* geometry. The unstability of the *trans* isomers was already attributed in earlier literature to the expected unfavorable interaction of the α hydrogens in the opposing bidentate ligands [18a,18f]. The idea seemed to be well founded in the light of the relative little amount of examples of *trans* complexes.

When obtained in *trans* geometry, complexes generally show a significant distortion of the coordination sphere in the N₄ equatorial plane. Two main types of distortion have been found experimentally: [18a–d] the *twisted* and
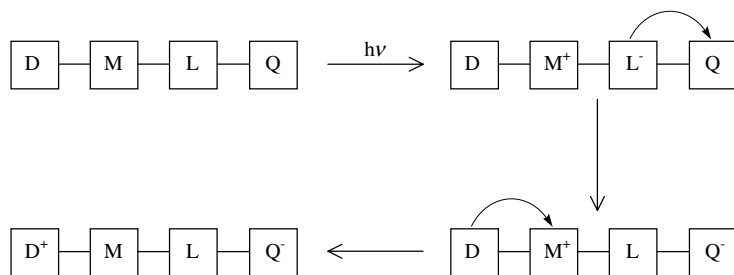
Scheme 4.

the *bowed* configurations. In the *twisted* configuration, each N–N is planar, but twisted out from the equatorial plane of the hexacoordinated metal. In the *bowed* geometry each N–N ligand is bent, i.e., the ligand loses planarity, and the equatorial plane is distorted in such a way as to minimize the opposing hydrogen interactions.

The thermal substitution reactions of photochemically generated *trans*-Ru(bpy)$_2$(OH)$_2$ appears to offer the most general and efficient synthetic route to obtain *trans* complexes. The electronic spectra of the complexes obtained show a general trend: [18a] the MLCT charge-transfer bands for the *trans* isomers appear at lower energies than those of the corresponding *cis* isomers. The Ru(III)/Ru(II) reduction potentials also show a consistent trend in that the *trans* isomers are oxidized at similar or less positive potentials than the corresponding *cis* isomers. Both of these observations suggest a stabilization of the dπ levels and a lowering of electron density at the Ru(II) center in the *cis* isomers relative to those in the *trans* isomers. A similar behaviour was observed for complexes obtained with the more rigid phen instead of bpy [18b].

3.2. Advantages of trans-geometry in [Ru(N–N)$_2$L$_1$L$_2$]$^{0,n+}$ type complexes

If the goal is to obtain long lived charge separate states following MLCT excitation, the incorporation of donor and/or acceptor substituents is a logical strategy.

Scheme 5 shows in a pictorial way the incorporation of donor (D) and acceptor (A) substituents on opposite (N–N) ligands for the *cis* and *trans* derivatives.

After light excitation through a MLCT band, a charge separate state should emerge, with the acceptor center bearing a negative charge, and the donor a positive. The photochemically produced redox equivalents are closer in the *cis* than in *trans* complexes. Therefore, through space back electron transfer is slowed down in *trans* complexes compared to the *cis*, and thus the corresponding excited state lifetime should enhance. The advantage of acquiring the *trans* geometry for these types of complexes makes itself evident.

Before discussing the way to favor *trans* geometry, it must be mentioned that a route for the preparation of *axial* asymmetrically functionalized *trans*-[Ru(bpy)$_2$L$_1$L$_2$]$^{n+}$ complexes was demonstrated. In it, pyridyl ligands bearing substituents in position 4 were sequentially introduced. For example, L$_1$ = Et-py (donor) and L$_2$ = COOEt-py (acceptor) were used [18d]. A more sophisticated type of chromophore-quencher complexes was subsequently synthesized and studied [18e]. Scheme 6 shows one example. The bulkiness of the axial ligands may contribute to maintain *trans* configuration. Nevertheless, visible light irradiation of the complexes led to photochemical decomposition. The presence of low lying photochemically reactive ligand field states was assigned as the possible reason for this decomposition. As a result, significant formation of charge separated states by electron transfer was not observed.
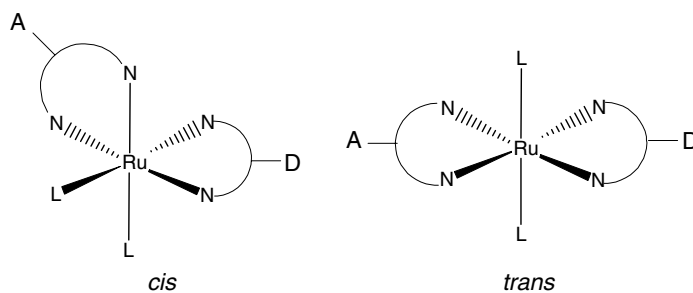
Scheme 5.
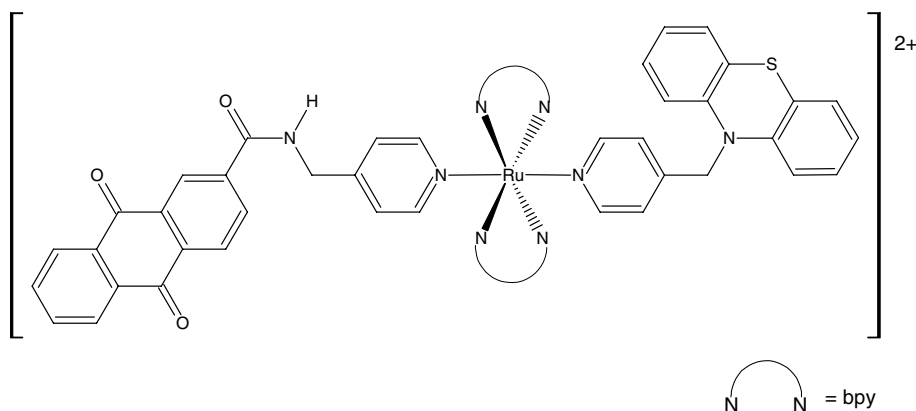
Scheme 6.

Returning to the understanding of the *cis–trans* problem in [Ru(N–N)$_2$L$_1$L$_2$]$^{0,n+}$ complexes, and to the challenge to obtain a *trans*-complex, two approaches were undertaken. First, a theoretical study on [Ru(phen)$_2$L$_2$]$^{n+}$ complexes was done, in order to understand the probable reasons for the preference of *cis* over *trans* geometry, and to deduce conditions that experimentally could favor the *trans* isomer formation. Second, and based on this, strategies to obtain *trans* complexes based on tetradentate ligands were proposed and experimentally tested.

3.3. Theoretical approach [18c]

The origin of the distortion in the equatorial N$_4$ plane of *trans*-[Ru(phen)$_2$L$_2$]$^{n+}$ type complexes was analyzed. The potential energy surface for complexes with different L ligands was explored. Starting from different initial geometries, the optimization procedure[5] led to the two experimentally observed distorted geometries (*twisted* and *bowed*) already mentioned, as well as to the absolutely planar configuration. Based on theoretical calculations, the latter is not a ground state geometry but a transition state, explaining in this way the absence of this configuration in experimentally characterized *trans* complexes. It should correspond to a connecting path among the *twisted* and the *bowed* distorted structures. The *bowed* configuration is more stable than the *twisted* in most cases, although the energy difference between both ground state minima is rather small. The energy barrier to go from one form to the other is also low, at least in the gas phase, but is sensitive to the axial ligand used. Regarding NH$_3$ or NH$_2$OH, higher barriers are obtained for L = F$^-$ and Cl$^-$. To understand fully the tendency observed for the barrier, and to understand the preference of *trans* complexes to adopt a distorted geometry, calculations were performed in order to separate different possible contributions to the barrier. An interaction between the axial NH$_3$ type ligands with the equatorial α hydrogens was invoked as the origin of the barrier lowering for this ligand. The role of the metal was also analyzed. The results show that although the repulsion between the equatorial α,α′ hydrogens definitely is an important factor to explain the preference for a distorted geometry in these complexes, its importance seems to have been overestimated in the literature, disregarding the other cited contributions.

Having understood the possible reasons for *trans* complexes to distort from planar geometry, the *cis–trans* problem was energetically studied. The total energy difference between the more stable *trans* geometry (*bowed*), and the

corresponding *cis*, $\Delta E_{trans–cis}$ was calculated. $\Delta E_{trans–cis}$ shows a dependence on the L ligand field strength, represented by Jorgensen's *f* ligand field parameter: although the *cis* isomer is generally more stable, weaker ligand fields tend to diminish the energy difference between both isomers. Other energetic calculations at ZINDO/S level were also performed, corroborating the general thermodynamic trend in favor of the *cis* geometry [18c]. Nevertheless, the energetic (thermodynamic) analysis described seems insufficient to justify the extremely marked preference of [Ru(phen)$_2$L$_2$]$^{n+}$ type complexes to adopt *cis* configuration. Therefore, a *kinetic* theoretical study was undertaken. The model was based on the synthetic route, in the sense that when a ruthenium salt (e.g., RuCl$_3 \cdot n$H$_2$O) reacts with phen ligand molecules, probably *one* phen coordinates first, and then the second. Starting from the optimized geometry for *trans* and *cis*-[Ru(phen)$_2$(CH$_3$CN)$_2$]$^{2+}$ complexes, a coordinate driving of the distance from ruthenium to *one* of the N atoms of *one* phenanthroline was performed. The initial point was the equilibrium Ru–N distance (~2.1 Å), and the last one a value of 5.3 Å, where the Ru–N distance is sufficiently long to assume bond breaking. Eight steps were considered, and the geometry of each step was fully optimized. The calculation sheds light of the inverse process, i.e., to the barrier that should generate when a phen ligand *approaches* a [Ru(phen)(CH$_3$CN)$_2$]$^{2+}$ moiety. The resulting potential energy diagram is shown in Fig. 6. It can be seen that the energy barrier to form the *trans* isomer is considerably higher than that to form the *cis*. Also, it is observed that the maximum appears at 4.4 Å for both isomers, indicating that barriers are mainly electrostatic in character. Finally, ab initio local hardness calculations using HF/3-21G* on [Ru(phen)(CH$_3$CN)$_4$]$^{2+}$ and phen, and HSAB criteria, corroborated the preference of *cis* coordination for the second phenanthroline.

Summing up the results of the theoretical analysis, the thermodynamic differences between the *cis* and *trans* isomers are not sufficiently pronounced to justify the definite experimental preference to form the *cis* isomer. The kinetic factor seems definitely to be more determinant.
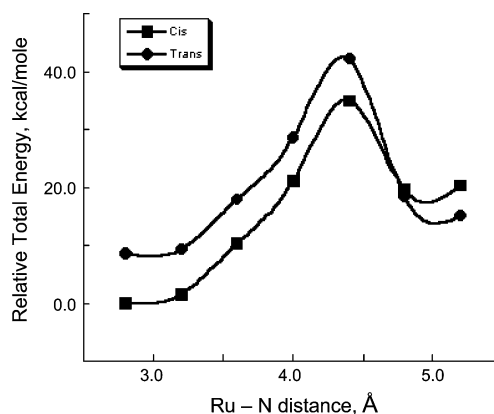

Fig. 6. Kinetic barrier for the formation of *cis*- and *trans*-[Ru(phen)$_2$(CH$_3$CN)$_2$]$^{2+}$ complexes from [Ru(phen)(CH$_3$CN)$_2$]$^{n+}$ and phenanthroline.

---

[5] Geometry optimizations were performed by using PM3(tm) semi-empirical methods as implemented in the Spartan package [19a]. Equilibrium geometries were checked for some cases by means of DFT ab initio calculations (B3LYP) and by comparison with crystallographic data, when available. More recently, all geometries were optimized using DFT methods (B3LYP, LACVP* basis set) as implemented in Titan [19d].
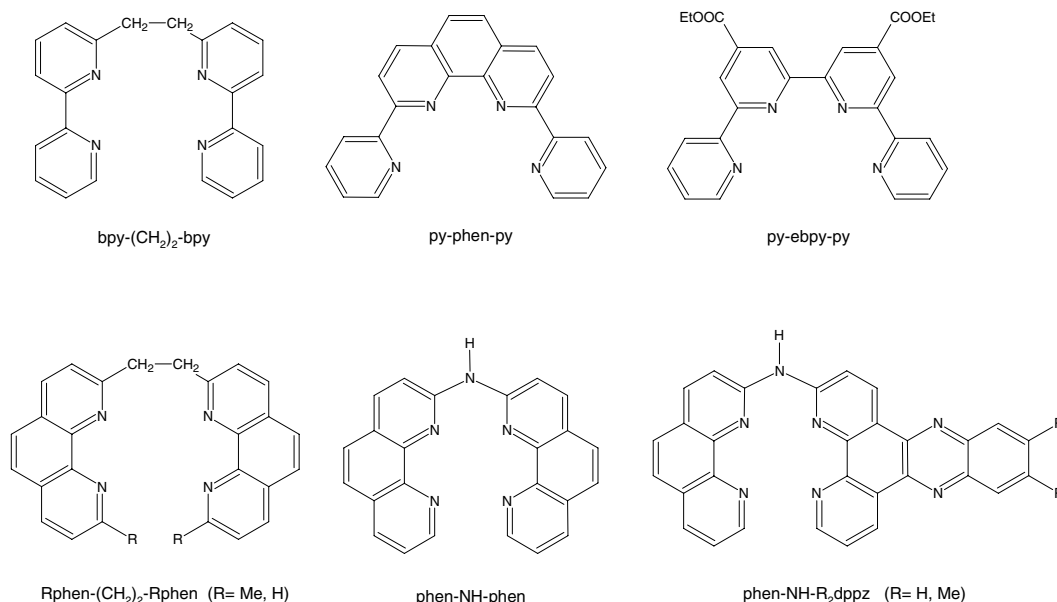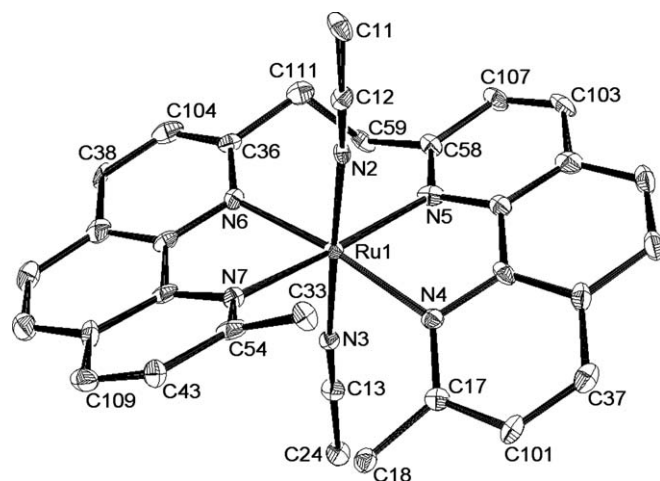
Fig. 7. Tetradentate ligands.

3.4. Forcing trans geometry: tetradentate ligands [19]

Given the theoretical analysis described above, the possibility to use tetradentate ligands to achieve *trans* geometry by avoiding the mentioned kinetic aspects was considered. The use of these types of ligands has the advantage of retaining many of the electronic features associated with the presence of bpy units [19d]. Ruthenium complexes with the ligand 1,2-bis-(2,2′-bipyridyl-6-yl)ethane, bpy–$(CH_2)_2$–bpy,[6] Fig. 7, had already been proposed more than a decade ago [19d,19e]. A series of *trans*-[Ru(bpy–$(CH_2)_2$–bpy)L_1L_2]$^{n+}$ complexes were prepared [19d]. For $L_1 =$ CH_3CN and $L_2 = Cl^-$, a distorted tilt geometry[7] with angle of 7.7° was observed. Interestingly, the lifetime values of *trans*-[Ru(bpy–$(CH_2)_2$–bpy)$(CN)_2$] and *cis*-[Ru(bpy)$_2$(CN)$_2$] are comparable: $\tau = 0.20$ μs (CH_2Cl_2) for the former, and 0.24 μs (CH_3CN) or 0.54 μs ($CHCl_3$) for the latter.

Modifications of this ligand, Rphen–$(CH_2)_2$–Rphen, R = Me, H, Fig. 7, were prepared. As discussed earlier in this paper, the more rigid phenanthrolines should enhance the excited state lifetime, according to the energy gap law. The ligand with R = Me was first reported by Lehn et al. [19j], but to our knowledge, the ligand with R = H had not been reported earlier. Four complexes were prepared: *trans*-[Ru(Mephen–$(CH_2)_2$–Mephen)$(CH_3CN)_2$]$(PF_6)_2$ (**1**), *trans*-[Ru(phen–$(CH_2)_2$–phen)$(CH_3CN)_2$]$(PF_6)_2$ (**2**), *trans*-[Ru(Mephen–$(CH_2)_2$–Mephen)$(CN)_2$] (**3**), and *trans*-[Ru(phen–$(CH_2)_2$–phen)$(CN)_2$] (**4**). The crystal structure of compound **1** is shown in Fig. 8. As opposed to *trans*-[Ru(bpy–$(CH_2)_2$–bpy)$(CH_3CN)_2$]$(PF_6)_2$ [19d], the absence

Fig. 8. Crystal structure of compound *trans*-[Ru(Mephen–$(CH_2)_2$–Mephen)$(CH_3CN)_2$]$(PF_6)_2$.

of a crystallographic inversion center at ruthenium results in a distinction between the bridged and opened sides of the tetradentate ligand. The phenanthroline moieties adopt a bowed configuration [18b,18c] and are significantly bent due to repulsion between the methyl groups (C18–C33 = 3.234 Å). The structure of compound **2** shows a higher degree of distortion. In the equatorial plane, the Ru–N distances of the open side of the ligand (2.092 and 2.045 Å) are considerably shorter than the corresponding for the bridged side: 2.135 and 2.100 Å. Nevertheless, the phenanthrolines display a higher degree of planarity, when compared with compound **1**. This is attributed to the presence of sterically less hindered H atoms in the opened side of the ligand.

The absorption spectra of **1** and **2** in acetonitrile display the typical pattern of a Ru(bpy)$_2$X$_2$ type compound

---

[6] Formely called *o*-bpy [19d].

[7] The tilt geometry is a special case of the bowed with a minumun distorsion [18c].

with two MLCT maxima at ~360–380 nm and at ~450 nm. Both compounds reveal no emission at room temperature (RT). They undergo photosubstitution by cyano ligands in acetone solutions to yield compounds **3** and **4**. This result is indicative of MLCT-dd crossing, possibly the main decay pathway for the excited state for compounds **1** and **2**. The presence of the stronger cyano ligands in axial positions increases the energy of the ^{3}MC excited states, resulting in a higher thermal barrier for the MLCT-dd crossing [19c]. When excited at 500 nm, complexes **3** and **4** display red luminescence in oxygen-free ethylene glycol at RT with maxima at 625 nm. In both cases the emission decay is bi-exponential. Time-resolved emission (TRE) studies for complex **3** revealed a blue-shift of the emission maximum from 625 nm to 616 nm after excitation in ethylene glycol. This behaviour is independent of the excitation energy. The decay lifetime have contributions from a fast and a slow component: 285 ns and 2300 ns for compound **3**, Fig. 9, and 18 ns and 546 ns for compound **4**.

In oxygen-free DMF the emission maxima for both complexes peaks at 662 nm. In this solvent, complex **3** displays lifetimes of 102 and 1104 ns for the fast and slow components of the decay, respectively. The pronounced red shift in the emission maxima from ethylene glycol to DMF, implies a change in symmetry from the ground to the excited state, which points towards electronic localization in one of the two phenanthrolines in the excited state. Work is in progress to study the C–N stretching vibration of the cyano ligands with TRIR to gain more information on the localization or delocalization of the excited electron. Further studies are also underway (transient absorption, low temperature emission) to determine the origin of the bi-exponential decay.

A tentative explanation for the bi-exponential decay can be suggested [19c]. In the ground state, the *bowed* configuration is the more stab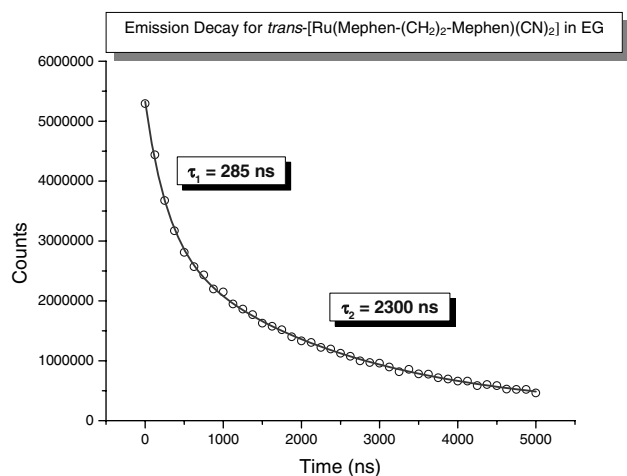le, as predicted by DFT calculations and further supported by the X-ray structures of **1** and **2**. In the excited ^{3}MLCT manifold, the *twisted* configuration is the more stable, although the *bowed* may also exist at higher energy. According to the photochemical reactivity observed, a metal centered state, MC, probably also exists, with an energy between the *twisted* and the *bowed* excited states, Fig. 10.

Thus, the excitation of molecules **3** and **4** in ethylene glycol turns the molecule from a *bowed* ground state to a *bowed* excited state. The *bowed* ^{3}MLCT excited state so formed possesses enough vibrational energy to thermally populate the ^{3}MC excited state. From the distorted ^{3}MC state the low-lying *twisted* ^{3}MLCT state is readily accessible and a Boltzmann distribution is established between these three excited states. The *twisted* excited state is probably strongly coupled to the ground state and decays very fast. Once thermal equilibration is reached, the ^{3}MC is no longer accessible and only the slow decay from the *bowed* excited state is observed. The decay in DMF is faster than in ethylene glycol due to the smaller effective energy gap in DMF. Further work, mainly temperature dependence studies, are in progress to test the presence of both configurations – *bowed* and *twisted* – thermally equilibrated in the excited state.

The considerable longer lifetime of compound **3** in regard to compound **4** in ethylene glycol can be understood in terms of the coordinate displacement ΔQ_e, Eq. (2). In **3**, the repulsion between the methyl groups in opposed phenanthrolines introduces rigidity in the molecule. In contrast, the presence of protons in this position in compound **4** introduces flexibility in the molecule, which enhances non-radiative decay to the ground state, and therefore a shorter lifetime. Using DFT (B3LYP, LACVP*) calculations [19k], the ratio S_4/S_3, with S defined in Eq. (2), was estimated to be 7.2, indicating a greater distortion in **4**, and, therefore, supporting the above-mentioned analysis.

Fig. 9. Emission decay for *trans*-[Ru(Mephen–(CH$_2$)$_2$–Mephen)(CN)$_2$] in ethylene glycol at RT.
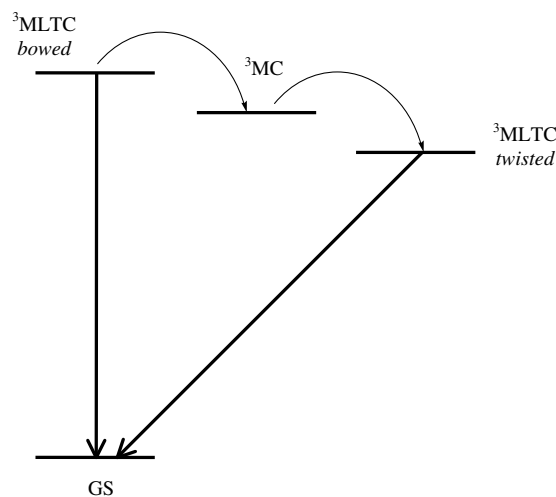

Fig. 10. Qualitative diagram of the excited state dynamics for **3** and **4** in ethylene glycol.

Regarding literature reports on tetradentate ligands, more recently the tetradentate 2,9-di-(2′-pyridyl)-1,10-phenanthroline, py–phen–py, Fig. 7, was reported [19f]. It has the property to induce mononuclear tetradentate coordination. The crystal structure of the [Ru(py–phen–py)(4-NMe₂py)₂]²⁺ with the axial ligand 4-dimethylami-nopyridine = 4-NMe₂py, showed a highly distorted but well organized structure, with a torsion angle of only −0.2(2)° for the N in the equatorial plane. In the ¹H NMR a notable deshielding of the protons in the distal pyridines of py–phen–py was observed, reflecting that on coordination this protons are pushed close to one another [19f]. Variation of the 4-substituent on the axial pyridines for methyl or CF₃ instead of 4-NMe₂ exerts a strong effect on the spectroscopic properties. A series of MLCT bands appear in the spectra of all complexes, with the long-wavelength bands assigned to MLCT transitions to the more electronegative py–phen–py ligand. These bands are strongly affected by the axial ligands, where electron-donating substituents destabilize the d-level ($\lambda_{max} = 580$ nm for NMe₂) relative to electron withdrawing substituents ($\lambda_{max} = 516$ nm for CF₃). Cyclic voltammetry measurements corroborate the influence of the axial ligand substitutions on the d-orbital energy. All complexes were not emissive at room temperature and 77 K. The observation was explained invoking the weak ligand field associated with the highly distorted coordination geometry. The distortion causes a lowering of the d–d states, which provides an alternate pathway for depopulation of the excited state. A similar argument was used to explain the lack of room temperature lumi-nescence for the less distorted [Ru(tpy)₂]²⁺, with tpy = 2,2′:6′,2″-terpyridine [19f,19h].

3.5. Asymmetric tetradentate ligands: a synthetic challenge

One further synthetic challenge was to obtain asymmetric tetradentate ligands [19a]. A complex with different polypyridyl moieties in the equatorial plane would have the additional advantage of generating donor and acceptor centers, which should increase the photoinduced charge separation capacity of the molecule. The idea then is to impose donor–acceptor centers in opposite equatorial positions, in order to take advantage of the seeked *trans* condition. The synthetic challenge is high, considering the need to couple two different moieties. Ogawa and Goto [19i] reported the synthesis of the ligand N,N-bis(1,10-phenan-throline-2-yl)amine, phen–NH–phen, Fig. 7, by the condensation of 2-NH₂-1,10-phen and 2-Cl-1,10-phen. To our knowledge, no complexation chemistry had been reported for this ligand. The same synthetic procedure was applied in order to obtain the asymmetric tetradentate ligands, phen–NH–dppz, phen–NH–ppl and phen–NH–dppz–Me₂ by coupling two *different* polypyridinic fragments, Scheme 7.

The *trans*-[Ru(phen–NH–phen)L₁L₂]⁰,²⁺ with L₁ = L₂ = Cl⁻, CH₃CN or DMSO and L₁ = CH₃CN, L₂ = DMSO were synthesized. Crystal structure determination was possible for L₁ = L₂ = CH₃CN and for L₁ = CH₃CN, L₂ = DMSO [19a]. In the latter, considerable distortion is observed due to both the unsymmetrical axial substitution and to the different Ru–N distances to the opened and to
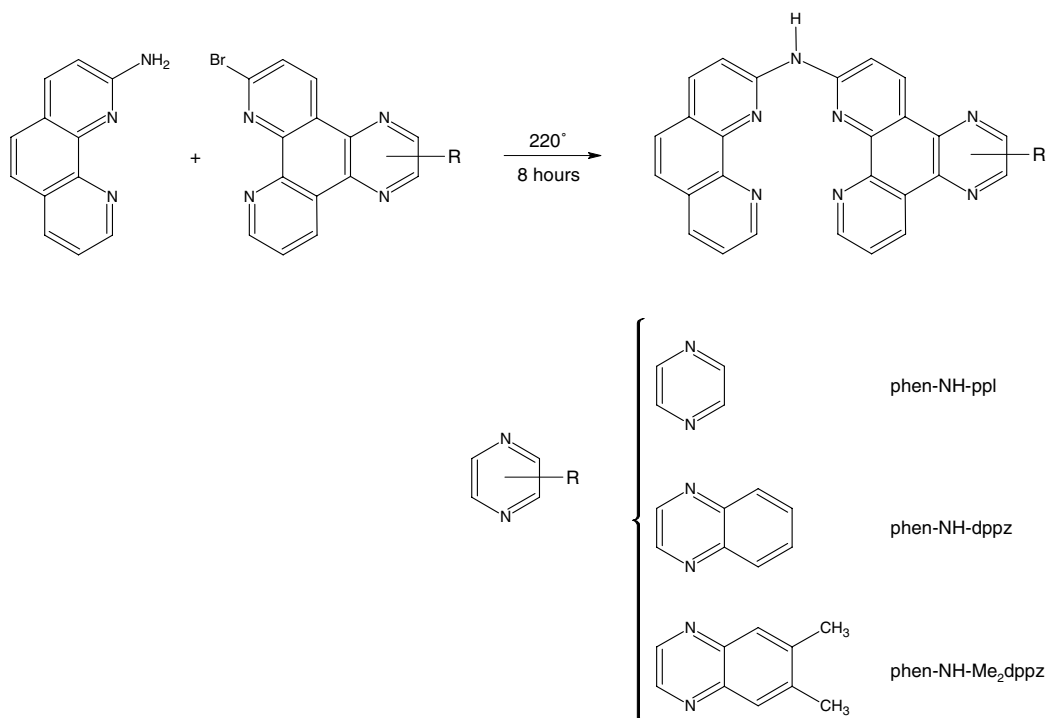
Scheme 7.

the closed side of the tetradentate ligand. The steric repulsion between the α hydrogens in opposite phenanthrolines is relieved by forming a higher angle to the open part of the ligand, allowing the phenanthrolines to be planar, tilted in respect to each other by an angle of 10.11°. A similar arrangement was reported for the complex [Ni(diphen)-(H₂O)Cl]Cl [19l]. On the contrary, for the compound with identical CH_3CN axial ligands, the opened side and the closed side of the ligand appear equivalent because of disorder generated by an opposite stacking arrangement of both sides of the ligand in the crystal, with an inversion center at ruthenium. The phenanthrolines appear rigorously planar.

With the asymmetric ligands the trans-[Ru(phen–NH–L)(OTf)₂], trans-[Ru(phen–NH–L)(CH₃CN)₂](PF₆)₂, trans-[Ru(phen–NH–L)(CN)₂] (L = ppl, dppz [19a], dppz-Me₂) complexes were prepared. The compounds were characterized by ¹H NMR, UV–Vis, IR and elemental analysis. Fig. 11 shows ¹H NMR spectra in CD_3CN for trans-[Ru(phen–NH–phen)(CH₃CN)₂](PF₆)₂ (**I**), trans-[Ru(phen–NH–ppl)(CH₃CN)₂](PF₆)₂ (**II**) and trans-[Ru(phen–NH–dppz)(CH₃CN)₂](PF₆)₂ (**III**). The presence of the asymmetric ligands in spectra **II** and **III** makes itself evident.

When excited at 450 nm, the four cyano complexes display emission in ethylene glycol. TRE studies revealed a red-shift of the emission maxima for trans-[Ru(phen–NH–dppz)(CN)₂], trans-[Ru(phen–NH–ppl)(CN)₂] and trans-[Ru(phen–NH–dppz–Me₂)(CN)₂] but not for trans-[Ru(phen–NH–phen)(CN)₂]. A possible explanation for this result is the presence of a non-negligible barrier between the higher energy, phenanthroline-based ³MLCT and the lower-energy, pyrazine-based ³MLCT. This explanation is supported by DFT theoretical calculations (B3LYP, LACVP* basis set). The LUMO of the complexes
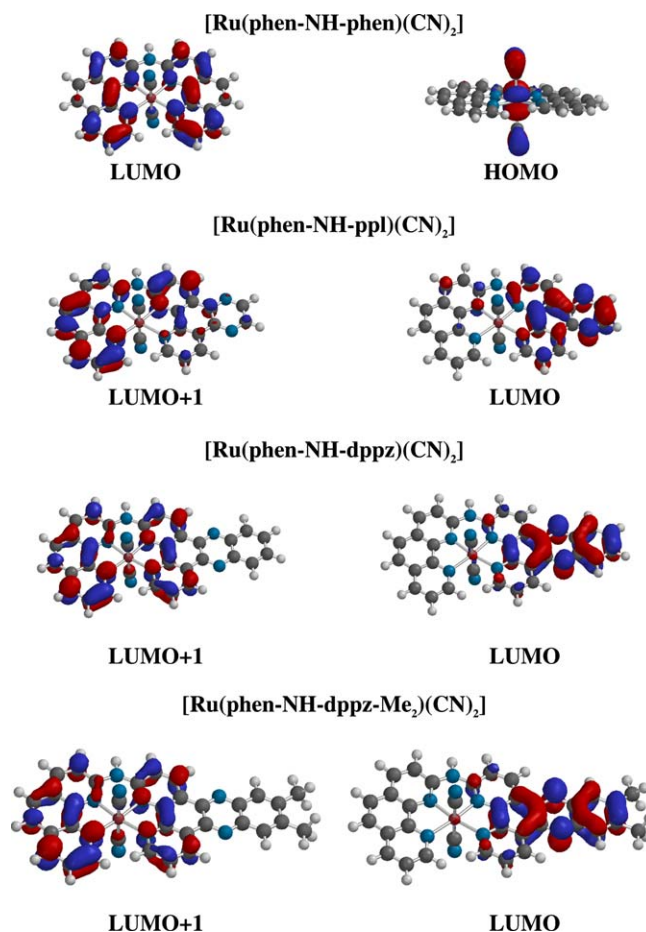

Fig. 12. Electronic distributions for the HOMO, LUMO and LUMO + 1 of some tetradentate complexes.

is localized in the pyrazine fragment and the LUMO + 1 is localized in the phenanthroline portions, with the exception of trans-[Ru(phen–NH–phen)(CN)₂]. For the later, the
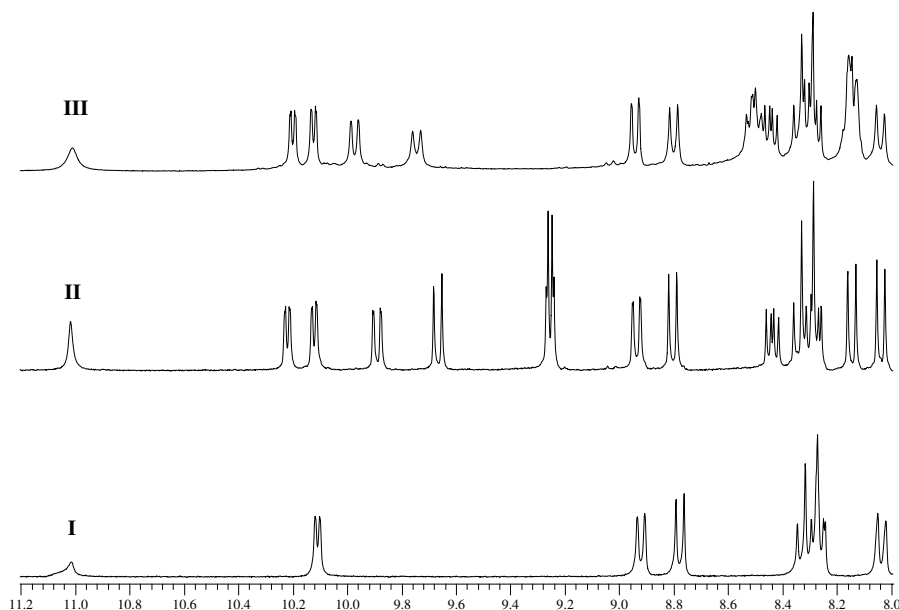

Fig. 11. ¹H NMR spectra in CD_3CN for tetradentate complexes **I**, **II** and **III**.

LUMO is delocalized over the entire ligand framework. Typical examples are shown in Fig. 12.

Decay traces in ethylene glycol following excitation at 450 nm, together with fittings to mono or bi-exponential decays for all complexes were registered. *trans*-[Ru(phen–NH–phen)(CN)$_2$] decays monoexponentially, as opposed to the rest of the complexes which decay bi-exponentially. For the latter case, initial population of the phenanthroline-based ^{3}MLCT together with the presence of a non-negligible barrier for the internal conversion to the lower energy pyrazine-based ^{3}MLCT, results in emission from both excited states. The higher energy, phenanthroline-based ^{3}MLCT decays faster because an important fraction of the excited molecules undergo internal conversion to the pyrazine-based ^{3}MLCT. Interestingly, the lifetimes of the excited states are almost identical for all the complexes with asymmetric ligands. But this is not surprising because in all three cases the nature of the lowest lying excited states is basically the same: a higher energy, phenanthroline-based ^{3}MLCT and a lower energy, pyrazine-based ^{3}MLCT. Further studies are in progress to better understand the excited state behaviour of these complexes.

4. Final comment and prospect

Different strategies for tuning the excited state properties of polypyridinic complexes by varying ligand structure and molecular geometry were described. Bidentate and tetradentate ligands based on fragments as dppz and ppl have been used. Future goals include the incorporation of *fused* quinonic moieties on tetradentate ligands, in order to put together both strategies described in this review to enhance excited state lifetime.

Acknowledgments

References

[1] (a) A. Juris, F. Balzani, F. Barigelleti, S. Campagna, P. Belser, A. von Zelewsky, Coord. Chem. Rev. 84 (1988) 84;
(b) T.J. Meyer, Pure Appl. Chem. 58 (1986) 1193;
(c) K. Kalyanasundaram, Photochemistry of Polypyridine and Porphyrin Complexes, Academic Press, London, 1992.
[2] R.J. Watts, J. Chem. Educ. 60 (1983) 834.
[3] (a) E.M. Kober, J.L. Marshall, W.J. Dressick, B.P. Sullivan, J.V. Caspar, T.J. Meyer, Inorg. Chem. 24 (1985) 2755;
(b) R.M. Leasure, L.A. Sacksteder, D. Nesselrodt, G.A. Reitz, J.N. Demas, B.A. DeGraff, Inorg. Chem. 30 (1991) 3722.
[4] (a) B. Durham, J.V. Caspar, J.K. Nagle, T.J. Meyer, J. Am. Chem. Soc. 104 (1982) 4803;
(b) G.B. Porter, R.H. Sparks, J. Photochem. 13 (1980) 123;
(c) D.P. Rillema, C.B. Blanton, R.J. Shaver, D.C. Jackman, M. Boldaji, S. Bundy, L.A. Worl, T.J. Meyer, Inorg. Chem. 31 (1992) 1600;
(d) D.P. Segers, M.K. DeArmond, J. Phys. Chem. 86 (1982) 3768;
(e) G.H. Allen, R.P. White, D.P. Rillema, T.J. Meyer, J. Am. Chem. Soc. 106 (1984) 2613;
(f) K.R. Barqawi, A. Llobet, T.J. Meyer, J. Am. Chem. Soc. 110 (1988) 7751;
(g) P. Chen, S.L. Mecklenburg, T.J. Meyer, J. Phys. Chem. 97 (1993) 13126;
(h) P. Chen, E. Danielson, T.J. Meyer, J. Phys. Chem. 92 (1988) 3708;
(i) F.N. Castellano, T.A. Heimer, M.T. Tandhasetti, G. Meyer, J. Chem. Mater. 6 (1994) 1041;
(j) W.E. Ford, M.A.J. Rodgers, J. Phys. Chem. 98 (1994) 7415;
(k) F. Barigelletti, A. Juris, V. Balzani, P. Belser, A.J. von Zelewky, J. Phys. Chem. 91 (1987) 1095;
(l) W.J. Vining, J.V. Caspar, T.J. Meyer, J. Phys. Chem. 89 (1985) 1095;
(m) E.M. Kober, T.J. Meyer, Inorg. Chem. 21 (1982) 3967;
(n) K.A. Goldsby, T.J. Meyer, J. Inorg. Chem. 23 (1984) 3002;
(o) E. Danielson, R.S. Lumpkin, T.J. Meyer, J. Phys. Chem. 91 (1987) 1305;
(p) G.A. Crosby, Acc. Chem. Res. 8 (1975) 231;
(q) S. Sprouse, K.A. King, P.J. Spellane, R.J. Watts, J. Am. Chem. Soc. 106 (1984) 6647;
(r) J.N. Demas, J. Chem. Educ. 60 (1983) 803;
(s) K.W. Hipps, G.A. Crosby, J. Am. Chem. Soc. 97 (1975) 7042.
[5] J.A. Treadway, B. Loeb, R. Lopez, P.A. Anderson, R.F.R. Keene, T.J. Meyer, Inorg. Chem. 35 (1996) 2242.
[6] (a) E.M. Kober, T.J. Meyer, Inorg. Chem. 24 (1985) 106;
(b) J.V. Caspar, T.D. Westmoreland, G.H. Allen, P.G. Bradley, T.J. Meyer, W.H. Woodruff, J. Am. Chem. Soc. 106 (1984) 3492;
(c) K. Maruszewski, K. Bajdor, D.P. Strommen, J.R. Kincaid, J. Phys. Chem. 99 (1995) 6286.
[7] (a) K.R. Barqawi, Z. Murtaza, T.J. Meyer, J. Phys. Chem. 95 (1991) 47;
(b) L.A. Worl, R. Duesing, P.Y. Chen, L. Della Ciana, T.J. Meyer, J. Chem. Soc., Dalton Trans. (1991) 849;
(c) J.V. Caspar, B.P. Sullivan, E.M. Kober, T.J. Meyer, Chem. Phys. Lett. 91 (1982) 91;
(d) J.V. Caspar, T.J. Meyer, J. Phys. Chem. 87 (1983) 952;
(e) E.M. Kober, J.V. Caspar, R.S. Lumpkin, T.J. Meyer, J. Phys. Chem. 90 (1986) 3722;
(f) E.M. Kober, J.L. Marshall, W.J. Dressick, B.P. Sullivan, J.V. Caspar, T.J. Meyer, J. Inorg. Chem. 24 (1985) 2755;
(g) J.P. Claude, Dissertation for degree of Ph.D., University of North Carolina at Chapel Hill, 1995.;
(h) A. Delgadillo, Doctor in Science with mention in Chemistry Thesis, Pontificia Universidad Católica de Chile, 2004.;
(i) R. López, Doctor in Science with mention in Chemistry Thesis, Pontificia Universidad Católica de Chile, 1996.;
(j) S.M. Molnar, K.R. Neville, G.E. Jensen, K.J. Brewer, Inorg. Chim. Acta 206 (1993) 69;
(k) A.W. Wallace, W.R. Murphy, J.T. Petersen, Inorg. Chim. Acta 166 (1989) 47.
[8] (a) M.I.J. Polson, S.L. Howell, A.H. Flood, A.K. Burrell, A.G. Blackman, K.C. Gordon, Polyhedron 23 (2004) 1427;

(b) R.M. Leasure, L.A. Sacksteder, D. Nesselrodt, G.A. Reitz, J.N. Demas, B.A. DeGraff, Inorg. Chem. 30 (1991) 3722;

(c) P.J. Giordano, S.M. Fredericks, M.S. Wrighton, D.L. Morse, J. Am. Chem. Soc. 100 (1978) 2257;

(d) J.R. Schoonover, W.D. Bates, T.J. Meyer, Inorg. Chem. 34 (1995) 6421;

(e) R. López, B. Loeb, D. Striplin, M. Devenney, K. Omberg, T.J. Meyer, J. Chil. Chem. Soc. 49 (2004) 149;

(f) M.K. Brennaman, J.H. Alstrum-Acevedo, C.N. Fleming, P. Jang, T.J. Meyer, J.M. Papanikolas, J. Am. Chem. Soc. 24 (2002) 15094;

(g) V.W.-W.V. Yam, K.K.-W. Lo, K.-K. Cheung, R.Y.-C. Kong, J. Chem. Soc., Dalton Trans. (1997) 2067;

(h) N.J. Lundin, P.J. Walsh, S.L. Howell, J.J. McGarvey, A.G. Blackman, K.C. Gordon, Inorg. Chem. 44 (2005) 3551;

(i) C. Turro, S.H. Bossmann, Y. Jenkins, J.K. Barton, N.J. Turro, J. Am. Chem. Soc. 117 (1995) 9026;

(j) G. David, P.J. Walsh, K.C. Gordon, Chem. Phys. Lett. 383 (2004) 292;

(k) F. Baumann, W. Kaim, M.G. Posse, N.E. Katz, Inorg. Chem. 37 (1998) 658;

(l) J. Fees, W. Kaim, M. Moscherosch, W. Matheis, J. Klima, M. Krejcik, S. Zalis, Inorg. Chem. 32 (1993) 166.

 [9] (a) A. Delgadillo, P. Romo, A.M. Leiva, B. Loeb, Helv. Chim. Acta 86 (2003) 2110;

(b) J. Aldrich-Wright, I. Greguric, R. Vagg, K. Vickery, P. Williams, J. Chromatogr. A 718 (1995) 436;

(c) X. He, L. Wang, H. Chen, L. Xu, L.N. Li, Polyhedron 17 (1998) 3161.

[10] (a) L. López, Licenciate in Chemistry Degree Thesis, Pontificia Universidad Católica de Chile, 1994;

(b) H. Gafney, T. Strekas, D. Baker, J. Am. Chem. Soc. 109 (1987) 2691.

[11] R.S. Lumpkin, E.M. Kober, L. Worl, Z. Murtaza, T.J. Meyer, J. Phys. Chem. 94 (1990) 239.

[12] (a) C.M. Dupreu, J.K. Barton, Inorg. Chem. 36 (1997) 33;

(b) A. Arancibia, A.M. Leiva, B. Loeb, Bol. Soc. Chil. Quim. 45 (2000) 587.

[13] (a) R. López, D. Boys, B. Loeb, F. Zuloaga, J. Chem. Soc., Perkin Trans. 2 (1998) 877;

(b) R. López, B. Loeb, T. Boussie, T.J. Meyer, Tetrahedron Lett. 37 (1996) 5437;

(c) R. López, A.M. Leiva, F. Zuloaga, B. Loeb, E. Norambuena, K.M. Omberg, J.R. Schoonover, D. Striplin, M. Devenney, T.J. Meyer, Inorg. Chem. 38 (1999) 2924;

(d) R. Díaz, O. Reyes, A. Francois, A.M. Leiva, B. Loeb, Tetrahedron Lett. 42 (2001) 6463;

(e) J.W. Robinson, Practical Handbook of Spectroscopy, CRC Press, Boca Raton, FL, 1991, p. 133;

(f) R. Díaz, Doctor in Sciences with mention in Chemistry Degree Thesis, Universidad de Concepción, Chile, 2000.

[14] (a) S.L. Mecklemburg, B.M. Peek, J.R. Schoonover, D.C. McCafferty, C.G. Wall, B.W. Erickson, T.J. Meyer, J. Am. Chem. Soc. 115 (1993) 5479;

(b) J. Otsuki, H. Ogawa, N. Okuda, K. Araki, M. Seno, Bull. Chem. Soc. Jpn. 70 (1997) 2077;

(c) S.L. Mecklemburg, D.C. McCafferty, J.R. Schoonover, B.M. Peek, B.W. Erickson, T.J. Meyer, Inorg. Chem. 33 (1994) 2974;

(d) K.A. Opperman, S.L. Mecklemburg, T.J. Meyer, Inorg. Chem. 33 (1994) 5295;

(e) V. Goulle, A. Harriman, J.M. Lehn, J. Chem. Soc., Chem. Commun. (1993) 1034.

[15] (a) G.F. Strouse, J. Schoonover, R. Duesing, T.J. Meyer, Inorg. Chem. 34 (1995) 2725;

(b) J.A. Treadway, P. Chen, T.J. Rutherford, F.R. Keene, T.J. Meyer, J. Phys. Chem. A 101 (1997) 6824;

(c) P.Y. Chen, S.L. Mecklenburg, R. Duesing, T.J. Meyer, J. Phys. Chem. A 97 (1993) 6811;

(d) R.J. Shover, M.W. Perkovic, D.P. Rillema, C. Woods, Inorg. Chem. 34 (1995) 6421.

[16] (a) J.R. Schoonover, W.D. Bates, T.J. Meyer, Inorg. Chem. 34 (1995) 6421;

(b) W.D. Bates, Ph.D. Dissertation, University of North Carolina at Chapel Hill, 1994;

(c) R. López, B. Loeb, D. Striplin, M. Devenney, K. Omberg, T.J. Meyer, J. Chil. Chem. Soc. 49 (2004) 149.

[17] (a) A. Arancibia, J. Concepción, N. Daire, G. Leiva, A.M. Leiva, B. Loeb, R. del Río, R. Díaz, A. Francois, M. Saldivia, J. Coord. Chem. 54 (2001) 323;

(b) A. Arancibia, A.M. Leiva, B. Loeb, Bol. Soc. Chil. Quim. 45 (2000) 587;

(c) E. Batista, R.L. Martin, J. Phys. Chem. A 109 (2005) 3128;

(d) M.K. Brennaman, J.H. Almstrum-Acevedo, C.N. Heming, P. Jang, T.J. Meyer, J.M. Papanikolas, J. Am. Chem. Soc. 124 (2002) 15094.

[18] (a) J.L. Walsh, B. Durham, Inorg. Chem. 21 (1982) 329;

(b) P. Bonneson, J.L. Walsh, W.T. Pennington, A.W. Cordes, B. Durham, Inorg. Chem. 22 (1983) 1761;

(c) J. Concepcion, B. Loeb, Y. Simon-Manso, F. Zuloaga, Polyhedron 19 (2000) 2297;

(d) B.J. Coe, T.J. Meyer, P.S. White, Inorg. Chem. 32 (1993) 4012;

(e) B.J. Coe, D.A. Friesen, D.W. Thompson, T.J. Meyer, Inorg. Chem. 35 (1996) 4575;

(f) E.D. McKenzie, Coord. Chem. 6 (1971) 187.

[19] (a) J. Concepción, O. Just, A.M. Leiva, B. Loeb, W.S. Rees Jr., Inorg. Chem. 41 (2002) 5937;

(b) J. Concepción, Doctor in Science with mention in Chemistry Thesis, Pontificia Universidad Católica de Chile, 2002.;

(c) J. Concepción, O. Just, S. Link, B. Loeb, W.S. Rees Jr., M. El Sayed, in preparation.;

(d) Md.A. Masood, B.P. Sullivan, D.J. Hodgson, Inorg. Chem. 33 (1994) 4611;

(e) T. Garber, S. Van Wallendae, D.P. Rillema, M. Kirk, W. Hatfield, J.H. Welch, P. Singh, Inorg. Chem. 29 (1990) 2863;

(f) R. Zong, R. Thummel, J. Am. Chem. Soc. 126 (2004) 10800;

(g) T. Renouard, R.-A. Fallahpour, Md.K. Nazeeruddin, R. Humphry-Baker, S.I. Gorelsky, A.B.P. Lever, M. Graetzel, Inorg. Chem. 41 (2002) 367;

(h) J.R. Kirchhoff, D.R. McMillin, P.A. Marnot, J.-P. Sauvage, J. Am. Chem. Soc. 107 (1985) 1138;

(i) S. Ogawa, N. Goto, Kogyo Kagaku Zasshi 74 (1971) 83;

(j) J.-M. Lehn, R. Ziessel, Helv. Chim. Acta 71 (1988) 1511;

(k) J. Concepción, O. Just, S. Link, B. Loeb, W.S. Rees Jr., M. El Sayed, C. Bignozzi, R. Argazzi, in preparation.;

(l) C.R. Rice, K.M. Anderson, Polyhedron 19 (2000) 495.

[20] J.R. Schoonover, G.F. Strose, K.M. Omberg, R.B. Dyer, Comm. Inorg. Chem. 18 (1996) 165.

[21] W.D. Bates, P. Chen, D. Dattelbaum, E.J. Jones Jr., T.J. Meyer, J. Phys. Chem. 103 (1999) 5227.